IEEE Open Journal of
Intelligent Transportation
Systems

Received 25 January 2024; revised 14 May 2024; accepted 25 May 2024. Date of publication 7 June 2024; date of current version 2 July 2024.

Digital Object Identifier 10.1109/OJITS.2024.3411525

SenseNow: A Time-Dependent Incentive Approach for Vehicular Crowdsensing

LUIS G. JAIMES[1] (Member, IEEE), HARISH CHINTAKUNTA[2] (Member, IEEE), AND PANIZ ABEDIN[1] (Member, IEEE)

[1]Department of Computer Science, Florida Polytechnic University, Lakeland, FL 33805, USA

[2]Department of Engineering, MathWorks, Santa Clara, CA 95054, USA

CORRESPONDING AUTHOR: L. G. JAIMES (e-mail: ljaimes@floridapoly.edu)

ABSTRACT This paper presents an incentive mechanism for vehicular crowdsensing (VCS). Here, a platform selects a set of spots or Places of sensing Interest (PsI) and outsources the collection of data from these places. In particular, the platform is interested in collecting data from most of the PsIs (spatial coverage) at regular and well-spread time intervals (temporal coverage). Although spatial coverage is a natural by-product of this approach, our main focus is to reach temporal coverage. To this goal, we model the interaction between participants (vehicles) as a non-cooperative game in which vehicles are the players, and the time to sample at a given PsI is the players' strategy. Here, vehicles are rewarded for deviating from their pre-planned paths and visiting a set of PsIs. The rewarding formula is designed such that selfish vehicles trying to maximize their reward will collect high temporal coverage data. In particular, this paper analyses the effects of increasing the number of vehicle deviations on the utilities of both vehicles and the platform.

INDEX TERMS Vehicular Crowdsensing, Smart Mobility, Algorithmic Game Theory, Transportation Systems.

I. INTRODUCTION

THE CONVERGENCE of vehicular technology, data analytics, and crowd-driven data collection has given rise to the field of Vehicular Crowdsensing (VCS). This new data collection paradigm harnesses the ubiquity of vehicles equipped with sensors and smart technologies to collect a rich spectrum of data, ranging from traffic patterns and road conditions to environmental variables. VCS is revolutionizing our understanding of urban dynamics and transportation systems. However, the true potential of VCS lies not only in the sheer volume of data collected but also in this information's spatial and temporal dimensions [1].

The timeliness of data is increasingly important, especially in applications that require real-time decision-making, trend analysis, and the early detection of critical events and anomalies. Regular data collection at uniform time intervals holds the key to achieving temporal coverage, a concept that transcends beyond data frequency. Temporal coverage embodies the ability to capture changes and events in their full context, allowing for a comprehensive understanding of evolving scenarios [2].

The advantages of having data collected at regular intervals include but are not limited to time synchronization and data quality control. It facilitates temporal alignment across different locations. This alignment enables the study of data correlations, dependencies, and temporal patterns. It is especially important in scenarios where events or changes in one location may impact or be related to events in other locations. Having the ability to monitor with this level of temporal resolution allows monitoring events such as the Piney Point cascading disaster in Florida [3] in 2021, where a massive marine wave of red tide started to spread around the shores of Pinellas, Sarazota, Hillsboro, and Manati counties, causing the death of 1,600-plus tons of marine life. This phenomenon's synchronized time and spatial observation allowed scientists to discover the release of around 215 million gallons of wastewater from the Piney Point phosphogypsum stacks into Tampa Bay.

The review of this article was arranged by Associate Editor Abdulla Hussein Al-Kaff.

Another advantage of this data type is predictive analytics and data consistency. Data at regular intervals allows time series analysis and machine learning models to predict future trends. In addition, data with temporal regularity is critical to making meaningful comparisons and avoiding biased results. Applications of data with these characteristics include Environmental Monitoring: Air quality [4], water quality, noise levels [5], and other environmental parameters across different locations. Tracking pollution levels, identifying environmental trends, and implementing targeted interventions for environmental conservation.

Traffic Management: Data collected at uniform time intervals from various locations can help monitor and manage traffic congestion, optimize traffic signal timings, and identify traffic patterns and hotspots [6]. This is crucial for improving transportation systems [7] and reducing traffic-related problems.

Weather Forecasting: Consistent data collection at multiple locations is vital for meteorological applications [8]. Weather data collected at regular intervals, including temperature, humidity, and wind speed, contributes to accurate weather forecasting, early warning systems, and climate research.

Smart Cities: Monitoring energy consumption, waste management, public safety, and urban planning [9]. Optimizing city operations and enhancing the quality of life for residents [5].

Healthcare: Epidemiological studies, disease tracking [10], and healthcare resource allocation. It supports public health initiatives and early detection of health trends.

Agriculture: Monitoring crop growth, soil conditions, and weather patterns. This information aids in precision agriculture [11].

Wildlife Conservation: Monitor wildlife populations [12], migration patterns, and environmental changes.

Disaster Management: It provides real-time information on natural disasters, such as floods, earthquakes, and wildfires, helping authorities make timely decisions and deploy resources effectively [11].

Infrastructure Maintenance: Monitoring the infrastructure condition, such as bridges, roads [13], and pipelines. It facilitates predictive maintenance and prevents infrastructure failures.

Public Safety: Surveillance and emergency response enhances situational awareness [14], enabling rapid responses to incidents and improving public safety [15].

We address the problem of collecting data at regular time intervals from all the places of sensing interest in a given region by proposing an incentive mechanism for VCS that encourages participants to collect sensing samples from PsIs located in or out of vehicles' pre-plain trajectories at regular intervals.

The proposed approach incentivizes participants' vehicles to engage in a strategic competition by deviating from their pre-established trajectories and opting to visit and collect data from PsIs that optimize their utilities. We model this competitive landscape as a non-cooperative game in which participants' vehicles are the players, and both the time to collect a sensing sample and where to collect that sample constitute a participant's local strategy. Thus, the routes that result from these local strategic deviations and visits to their selected PoIs constitute the participants' strategic global choices. Through rigorous analysis, we demonstrate that no participant can independently enhance their utility by unilaterally deviating from their current strategies, thus illustrating the Nash equilibrium concept. Moreover, we highlight that the aggregation of participants' trajectories not only contributes to an augmented platform utility QoSD, but also results in improved spatial coverage, heightened road utilization, and an overall increase in the average participant's utility.

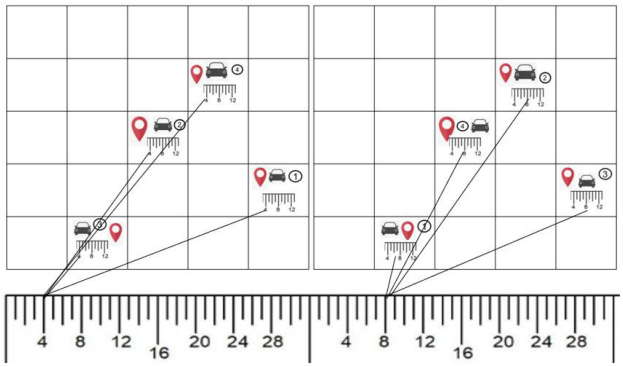

FIGURE 1. Vehicular Crowdsensing sketch.

Figure 1 depicts the fundamental elements of the proposed VCS system. The two main components are the platform and the participant vehicles. The platform administers a wide array of sensing tasks strategically dispersed across distinct locales of interest, hereafter denoted as Places of Sensing Interest (PsI). The platform also assigns a reward for the execution of each sensing task. These rewards attract participant vehicles who are incentivized by rewards and willingly divert from their predefined trajectories and head to the advertised PsIs to execute the sensing tasks. Here, each PsI is sampled regularly and the samples are collectively reported at that time. Thus, the platform has a big picture of what is happening at a given time in all the PsI (temporal coverage).

In this study, we operate on the premise that all vehicles function autonomously, with passenger decision-making processes excluded from consideration. Consequently, the terms "user," "participant," "player," "contributor," "AV" (Autonomous Vehicle), and "vehicle" are employed interchangeably throughout this research to denote the entities engaged in the VCS framework.

The followings items summarize the paper's main contributions:

- We present a VCS market in which time dependable sensing and temporal coverage drive the utilities of contributors and crowdsourcers.
- We formulate the VCS Temporal Coverage Nash equilibrium (NE) problem.

- We design a greedy iterative algorithm to approximate VCS Temporal Coverage NE.
- We evaluate our algorithms using a real-world traffic map, and the state-of-the-art traffic simulator SUMO

II. RELATED WORK

In this section, we briefly review and analyze the most related methods to our proposed approach.

Chintakunta et al. [2] propose an incentive mechanism for VCS that encourages participants to collect uniform distributed data in time, therefore optimizing time coverage. Here, vehicles are allowed to deviate once from their pre-planned trajectory, collect data, and head to their destination. In this work, we extend the aforementioned work by allowing participants to deviate more than once and analyzing the trade-offs in terms of time complexity versus improvements and platform and participant utilities. In 2015, Han et al. [16] proposed a vehicle selection algorithm that minimizes the vehicle's trajectory. They first developed an offline heuristic algorithm. Then, they improved their algorithm by considering the uncertainty of vehicle behaviors. Wang et al. [7] present a crowd-sensing system that maximizes spatial-temporal coverage. The authors' approach involves maximizing coverage through a smart combination of sub-segments from each vehicle trajectory. Unlike our system, this one focuses on public transportation, where trajectories are fixed and unable to cover locations beyond the vehicle's path.

Spatial and temporal variability is a critical aspect of data quality in crowd-sensing, and it poses unique challenges and considerations in ensuring the reliability and accuracy of data collected through crowd-sourced methods. Spatial variability refers to the differences in data quality across different geographical locations or regions. It arises due to various factors, including geographical coverage, environmental conditions, user expertise, etc [17]. Van Exel et al. [18] discussed the impact of crowdsourcing on spatial data quality indicators. Temporal variability, on the other hand, deals with changes in data quality over time. Key considerations include Data Aging, Temporal Sampling, Events, and Emergencies, User Engagement etc. Addressing temporal variability requires designing systems that encourage timely updates and provide mechanisms for verifying and validating data as it evolves. Maximizing spatial-temporal coverage is one of the important tasks to achieve high-quality crowd-sensing. Numerous studies have been conducted in this particular field [7], [19], [20], [21]. In this paper, our main focus is on temporal coverage. The rewarding formula is designed in such that selfish vehicles trying to maximize their reward will collect high temporal coverage data.

In crowdsensing, where individuals contribute data for collective insights, game theory can provide a framework for understanding and optimizing behavior. Lu et al. [22] demonstrate a game theory approach that establishes a client-server relationship among diverse users interacting with the server. The primary objective is to maximize the utility of the server with clients through various parameters. In contrast, this paper takes a simpler approach, using fewer variables to assess how each vehicle maximizes its utility. This deliberate simplification contributes to a more manageable problem-solving framework.

Reinforcement learning plays a pivotal role in enhancing incentive mechanisms within crowdsensing frameworks by enabling adaptive and dynamic adjustments based on the evolving behaviors of participants, thereby optimizing the overall efficiency and effectiveness of data contributions. In the work by Xue et al. [23], reinforcement learning was employed to address the prisoner's dilemma, aiming to incentivize long-term cooperation. The authors emphasize the need for a more intricate study beyond a two-user scenario. In this paper, we extend the complexity explored by their work by involving multiple users interacting with shared resources, providing a real-world example that amplifies the challenges and dynamics identified in their study.

Big data technologies are essential for managing the massive and complex datasets produced through crowd-sensing activities. Xu et al. [24] explain the significant big data capabilities inherent in the Internet of Vehicles, outlining its potential for collecting and storing data. Building upon this insight, the present study leverages these capabilities to introduce an innovative economic incentive for autonomous vehicles. This incentive system involves autonomous vehicles collecting revenue from Points of Interest, subsequently, benefiting the vehicle owner through the accumulated funds.

In this paper, we frame our research in data being collected and then given to the different Points of Interest around a city. In contrast to Kong et al.'s [25] utilization of fabricated data to generate trajectories navigating points of interest, our approach involves testing trajectories on real roads within actual cities. The points of interest chosen in our study closely mimic the distribution found in the real world, offering a more realistic representation of spaced-out points of interest.

As the role of crowdsensing in urban environments continues to evolve, researchers have explored diverse applications, from gathering road information during car journeys, as demonstrated by El-Wakeel et al. [13], to assessing noise pollution through citizen-driven data collection, exemplified by Maisonneuve et al.'s framework [5]. El-Wakeel et al. [13] illustrate the possibility of acquiring road-related information during a car's route to a destination. This study substantiates the feasibility of applying this concept to a more extensive fleet of vehicles and broader road network by incorporating destination points and points of interest throughout a city. Furthermore, Maisonneuve et al.'s framework [5], designed for measuring noise pollution, involves citizens using their mobile phones to collect data on personal exposure to noise in their daily surroundings. This research not only expands the practical applications of our work to the general public but also aligns with the comprehensive exploration of

crowdsensing's potential in public spaces, as emphasized by Chon et al. [9].

The increasing volume of information generated by a growing number of vehicles on the road underscores the necessity and relevance of research endeavors related to crowdsensing frameworks. Sun et al. [26] state that the rational of human drivers are irrational when making their own paths. They then devise a path that is bounded rationally from going one point to another. Unlike our paper, they do not consider the specifics of multi-point of interests. Our paper expands on the notion of automated pathing to maximize the utility of vehicles moving through multiple different points of interest.

Yang et al. [27] explain in a similar study that the best case for mobile crowdsensing is for the users to select what they are getting paid. This paper then expands on that idea by making it so that multiple vehicles can decide when and for how long they are at each point of interest thereby deciding how much they are getting by also optimizing the value of the overall system.

As vehicles have the advantages of predictable mobility, He et al. [28] focused on improving the crowdsourcing quality. They proposed a vehicle-based participant recruitment problem and provided approximation algorithms to maximize spatial, and temporal coverage subject to a limited budget k. Their approach considered the current and future locations of vehicles in a way that the quality of crowdsourcing for a period of time in the future can be guaranteed. Although their work is similar to our approach in terms of maximizing temporal and spatial coverage, they didn't consider vehicles deviating from their pre-planned trajectories. Similar to this approach, in 2019, Xu et al. [29] presented an incentivizing system to optimize the sensing coverage of collected data. Their work focuses on reducing the cost of incentivizing vehicles and utilizing the budget efficiently.

In addition to the above works, Urra and Ilarri [30] explain another framework to collect data from regular car's going from destination to destination with a mobile agent hoping between cars. Unlike our paper, their paper focuses on the ability to have cars going from place to place without the possibility of veering off course. This paper takes a broader view of the collection and assigns the car's their own local storage allowing more overall data to be transferred and collected. Chen et al. [31] conduct their research on the segmentation of crowdsensing data to better collect certain data from crowdsensing overall. Our paper, on the other hand, moves towards using the whole path to collect data and also to provide the greatest spatial coverage possible with all the vehicle participants, thus getting around their main focus which was to reduce redundancy.

There are various approaches to crowdsensing research, each with its unique data collection system. Kim et al. [32] focus on human participants going through their regular routes in order to contribute to an ongoing problem or to a data collection. Unlike our paper, the study had to take into account the participant's willingness through a more complex model because of dealing with human participants. This paper circumvents the problem by focusing on only the vehicle's willingness which is provided by mathematical formulas.

Fan et al. [33] investigate on how crowdsensing and spatial-temporal coverage can help drivers from the different apps get more out of their drive. Starace et al.'s [34] research which shows how much coverage a taxi service in an urban can cover. This paper then expands the usage space from just human drivers to any vehicle capable of driving, with or without human intervention. This paper addresses the issue by concentrating solely on the vehicle's willingness, as determined through mathematical expressions.

Gathering data passively with a planned route may preclude the system from maximizing the sensing coverage. Similar to our work, Zhu et al. [35] considered modifying the planned routes of participants while collecting data. Their platform uses a reverse auction to motivate participants to generate trajectories and bid for them. Once the platform receives proposals from participants, it selects the set of vehicles and proposed routes, which can maximize coverage. Although this is similar to our approach in the sense of reaching PsIs out of the vehicles pre-planned trajectories, it doesn't provide details about the incentive mechanism for data acquisition, the cost of participation, or any participant behavioral model.

The conceptualization of vehicular crowdsensing as a game represents a well-established research domain. This phenomenon introduces a game between users that form the participant pool, as well as between the participant pool and the Mobile Crowdsensing platform. Research on various game theoretic approaches aims to provide a stable solution to this problem [36]. Many incentive strategies have been suggested to motivate mobile users to engage in crowdsensing activities. Nevertheless, most of these methods distribute uniform rewards for sensing tasks and presume a consistent group of participants, disregarding the inherent variability in task importance and the unpredictable nature of participant arrivals. These factors have long been overlooked, particularly in time-sensitive and location-dependent crowdsensing environments. Wang et al. [37] addressed such limitations by concentrating on time-sensitive, location-dependent crowdsensing systems with random participant arrivals. They introduced a two-tiered heterogeneous pricing approach to distribute participant involvement across tasks equitably. Xiao et al. [38] directed their attention towards the influence of sensing task types on the efficiency of a VCS system. Here, the authors proposed a vehicular crowdsensing game wherein each participating vehicle formulates its sensing strategy contingent upon sensing cost, radio channel state, and anticipated remuneration. Their model introduces a game dynamic between the central platform and participating vehicles, wherein the accuracy of sensing reports serves as the participant strategy, while the payment policy constitutes the platform strategy. This framework resembles our research in high-level game design, precisely the pursuit of a

noise-free set of samples Nash Equilibrium. Nevertheless, a distinction arises in our focus, wherein our emphasis lies in the maximization of temporal coverage while visiting the PsIs situated beyond the pre-planned trajectories of the participants. In addition, Wang et al. [39] utilized game theory to formulate a multi-round bidding strategy where users compete for sensing tasks based on their available time and desired task quantity. Users dynamically adjust their bidding probabilities to reach a Nash Equilibrium, aiming to maximize task acquisition within their time constraints. Unline this multi-round bidding strategy. Duan et al. [40] focused on incentivizing smartphone users' collaboration for data acquisition and distributed computing applications. In this approach, a reward-based collaboration mechanism has been proposed, where a master announces a total reward to be distributed among collaborators, and successful collaboration occurs if a sufficient number of users opt to participate. In contrast, our approach incentivizes vehicles in vehicular crowdsensing scenarios to maximize temporal coverage of data collection from designated Points of Interest (PoIs). By modeling vehicle interaction as a non-cooperative game, participants are rewarded for deviating from their planned routes to visit PoIs, thereby enhancing temporal coverage. This incentivization mechanism encourages vehicles to prioritize data collection at critical times, ultimately improving collected data quality. Thus, while both approaches leverage game theory principles, our approach's emphasis on incentivizing behavior to enhance temporal coverage offers a unique advantage over their approach, potentially yielding more comprehensive and valuable crowdsensed data.

Next, we outline the fundamental components of our proposed method and the connections between them, aiming to offer a thorough insight into the structure and the details of our incentive mechanism framework.

III. SYSTEM MODEL

This section delineates the principal elements of our proposed approach and the interrelations among these to provide a comprehensive understanding of the incentive mechanism's structure and functionality. The entities involved in the proposed incentive mechanism are the platform and the participants (AVs). The platform's goal is to collect "high-quality" data from participants at the set of PsIs. For the purposes of this work, data quality is measured by the temporal diversity of the data. The optimal maximization of this metric (i.e., data quality) occurs when the sample points exhibit a uniform distribution throughout the observation time, thereby ensuring comprehensive temporal coverage.

The remainder of this section will formalize the notions of temporal diversity, the calculation of the reward, and the participant's decision-making process.

Autonomous vehicles (AVs) are given a reward of $R\delta$ per sample, where R remains constant, and the multiplier δ is carefully tweaked to enhance sample quality. This assumes that the AVs act selfishly and rationally, possessing full knowledge of other AVs' original trajectories. Each AV gains a reward for sample collection. However, there is an associated cost when an autonomous vehicle (AV) deviates from its pre-planned path. The parameter δ is contingent on the timing of the preceding sample, ensuring that when AVs opt for targets to optimize their utility (defined as the reward minus the cost), the resultant samples maintain a high level of quality. Thus, given the interdependence of autonomous vehicles (AVs) utility functions on the decisions of other AVs, the process of AVs selecting a PsIs to visit has the form of a competitive game. It is imperative that any selections made by AVs establish a Nash equilibrium,

Also, in order to simplify the task at hand, we make the following assumptions:

- Starting synchronously from their respective source locations, all vehicles initiate their trajectories simultaneously,
- Each vehicle alters its initial trajectory to visit a maximum of two PsIs,
- The vehicles do not halt at the PsIs, and the sampling time coincides with the time of arrival at the PsI. Section V explores potential modifications to the proposed mechanism in the event that these assumptions are not satisfied.

Subsequent to this introduction, we will proceed to formalize and quantify both the platform and participants' utility functions. Additionally, we will offer an intuitive rationale for the selection of these functions, explaining their correlation between the selection of participants' utility functions and subsequent maximization of the platform utility. Furthermore, we will sketch an algorithm that AVs can use to select PsIs strategically. Thus ensuring that collective choices of PsIs for all AVs result in a Nash equilibrium.

A. THE PLATFORM MODEL

The proposed system model includes M PsIs and N AVs. Where $T = \{t_1, t_2, \ldots, t_M\}$ is the set of PsIs, and $V = \{v_1, v_2, \ldots, v_N\}$ the set of AVs. At the core of our analysis is the concept of temporal coverage, which is quantified by the quality of the collected samples. The quality is ideally maximized when the collection times of the samples are uniformly distributed over time, meaning the intervals between consecutive samples are consistent (i.e., same length). We use the concept of entropy to assess the quality of set sensing samples. Consider a scenario where n samples are collected at a given PsI over an observation period T_o. This period is segmented into $n+1$ intervals, each denoted as $l_i, i = 1, \ldots n+1$. These intervals collectively sum up the total observation time $\sum_1^{n+1} l_i = T_o$. By normalizing each interval l_i with respect T_o, we obtain a set of probabilities $p_i = l_i/T_o$. It is crucial to note that these normalized intervals, p_i, range between 0 and 1. The sum of all p_i values equals 1, allowing these values to be interpreted as a probability distribution, which we denote as P. This probabilistic framework enables a more nuanced sample

distribution and quality analysis within the given system model.

When the sampling times associated with a set of collected samples follow a uniform distribution, the utility function, namely quality, is expected to reach its maximum value. Conversely, the least favorable scenario in terms of temporal coverage occurs when all samples are concentrated either at the onset or at the conclusion of the observation period. This distribution leads to a skewed probability profile, characterized by one of the probabilities being one while the others are reduced to zero. In such a situation, the utility function is anticipated to attain its minimum value. The value of the utility function is hypothesized to increase progressively as the sample distribution transitions from this suboptimal state toward the ideal uniform sampling condition.

This relationship is further quantified by the entropy function $E(P) = \sum_i p_i \ln \frac{1}{p_i}$, which represents the dispersion or uniformity of the sample points across the observation period. The entropy function, therefore, provides a critical measure for assessing the quality of temporal coverage based on the distribution of sample points within the given observation framework. Cover and Thomas [41] proved that $\sum_{i=1}^{n} p_i \ln(1/p_i i)$ is bounded by $\ln(n)$, reaching its apex when all probabilities p_is are equivalent, namely uniform inter-sample intervals.

The utility or quality of samples collected at PsI j corresponds to $\mathcal{U}_j = \sum_i p_i \ln \frac{1}{p_i}$. Where i are number of inter-sample intervals at j. Thus, the overall platform utility can be expressed as

$$\mathcal{U} = \frac{1}{M} \sum_{j=1}^{M} \left(\sum_{i=1}^{n} p_i \ln \frac{1}{p_i} \right), \tag{1}$$

B. AV MODEL

Each autonomous vehicle (AV) denoted as v_i follows a predetermined trajectory from its starting point, s_i, to its destination, d_i. The platform's primary objective is to motivate these AVs to diverge from their pre-established paths to gather high-quality samples at specific PsIs (Probabilistic Sampling Instances). To achieve this, the platform employs a reward mechanism, where a reward of $R\delta$ is assigned for each sample. Here, R remains a constant maximum reward, and δ is a variable multiplier that varies within the range of 0 to 1 and changes with each sample. The utility function for AV v_i regarding the collection of samples at PsI t_k can be expressed as follows:

$$u_i(t_k) = R\delta - \alpha(|s_i t_k d_i| - |s_i t_i|), \tag{2}$$

where $|s_i t_k d_i|$ is the distance of the path $s_i \to t_k \to d_i$, and $|s_i d_i|$ is the distance of the path $s_i \to d_i$. The value of α is used to regulate the cost of deviating and visit PsI t_k.

In this paper, we also consider the case where an AV is able to visit at most two PsIs before reaching the destination.

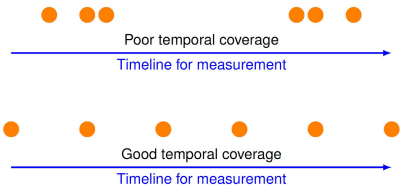

FIGURE 2. Poor vs High temporal coverage.

Thus, for the vehicle v_i, the utility function u_i for collecting samples at PsIs t_k and t_p is then given as

$$u_i(t_k, t_p) = R(\delta_k + \delta_p) - \alpha(|s_i t_k t_p d_i| - |s_i d_i|) \tag{3}$$

where, δ_k and δ_p are multipliers corresponding to PsIs t_k and t_p respectively. In other words, for n *PsIs* where $n = 0, 1, 2$. Thus, the participant's strategy would be to collect samples at one or two PsIs or not deviate from the original trajectory based on the following value.

$$\max\{u_i(t_k, t_p), u_i(t_k), 0\} \tag{4}$$

Equation (3) can be written as a function of the number of visited *PsIs*

$$u_i(t_n) = R(\delta_n) - \alpha|s_i t_n d_i| - |s_i d_i| \tag{5}$$

For $n = 0, 1, 2$, namely visiting zero, one, or two *PsIs*. Our focus now shifts to the δ parameter in Equation (2). The overarching aim of this model is to analyze temporal variations of sensing variables across an observation period. It is pertinent to acknowledge that successive samples collected in immediate time proximity typically yield minimal incremental analytical value.

Hence, the configuration of δ is strategically formulated to encourage a sampling pattern distributed across the observation timeline rather than clustered in narrow temporal segments, as shown in Figure 2. This approach is critical for ensuring a more comprehensive and varied data collection, enhancing the potential for insightful analysis.

In the proposed framework, we define a_{ik} as the arrival or sampling time of the Autonomous Vehicle (AV) v_i at PsI t_k. Further, a_{ik}^{-} is characterized as the time corresponding to the most recent sampling event at t_k, explicitly excluding any sampling by v_i. In scenarios where v_i represents the initial AV reaching t_k, the value of a_{ik}^{-} is set to $-\infty$. The parameter δ is expected to exhibit the following characteristics:

1) As $a_{ik} \to a_{ik}^{-}$, δ *approaches* 0.
2) As $a_{ik} - a_{ik}^{-} \to \infty$, δ *approaches* 1,
3) δ is a concave function of $a_{ik} - a_{ik}^{-}$ reflecting a diminishing rate of return with the increase in the sampling interval.

Here, the computation of δ is influenced by the choice or allocation of PsIs by other AVs, and the value of a_{ik}^{-}. Let v_j^* represent the PsI chosen by another AV v_j. Consequently, the parameter δ is dependent not only on $a_{ik} - a_{ik}^{-}$ but also on the choices $\{v_j^*\}, j \neq i$ made by all other AVs. An example of

a function for δ that exhibits the aforementioned properties is:

$$\delta\Big(a_{ik} - a_{ik}^{-}, \{v_j^*, j \neq i\}\Big) = 1 - e^{-\frac{a_{ik}-a_{ik}^{-}}{\tau}}, \tag{6}$$

Here, τ assumes the role of a controlling factor tunning the temporal gap between consecutive data samples. By using equations (2) and (6), we can formulate the utility function for AVs as follows:

$$u_i\Big(t_k, \{v_j^*, j \neq i\}\Big) = R\Big(1 - e^{-\frac{a_{ik}-a_{ik}^{-}}{\tau}}\Big) - \alpha(|s_i t_k d_i| - |s_i t_i|) \tag{7}$$

Thus, participant v_i will sample at the PSI v_i^* at the time that maxes out its profit.

$$v_i^* = \arg\max_{t_k} u_i\Big(t_k, \{v_j^*, j \neq i\}\Big), \tag{8}$$

Therefore, an assignment of AVs to PsIs in which equation (8) is satisfied for all the vehicles corresponds to a Nash Equilibrium.

Equations (6), (7), and (8) can be further generalized to consider two deviations. Specifically, an AV v_i will choose to visit a set of PsIs, V_i^*, if the combination if these PsIs maxes out its utility as shown in equation (3).

$$V_i^* = \arg\max_{t_k, t_p} u_i\Big(t_k, t_p, \{V_j^*, j \neq i\}\Big), \tag{9}$$

C. PSI ALLOCATION ALGORITHM

Equation (9) corresponds to a strategic game $G = \langle V, A, u_i \rangle$, where V is the set of vehicle players, $A = T^{|V|}$ is the joint action space of choices of PsIs available to each AV, and $u_i{:}A \rightarrow \mathbb{R}$ is a utility function representing the preferences of each player $i \in V$ over action profiles $a \in A$. Specifically, each AV v_i's utility function u_i determines its utility for choosing a particular set of PsIs $V_i^* \subseteq T$, given the PsI selections $V_j, j \neq i$, made by all other AVs. An action profile $a = (V_1, \ldots, V_N) \in A$ is a Nash equilibrium if no single AV i can gain higher utility by unilaterally changing its strategy, i.e.,

$$u_i(V_i, V_{-i}) \geq u_i\big(V_i, V_{-i}^*\big), \forall V_i \subseteq T, \forall i \in N \tag{10}$$

Thus, if a Nash equilibrium exists in G, rational AVs will choose their PsI allocations according to Equation (9), representing the equilibrium strategy profile.

Since each AV has $M(M-1) + M + 1$ possible PsI allocation strategies (visiting none, one, or two of the M available PsIs), the total number of possible joint PsI allocation profiles across N AVs is $(M(M-1) + M + 1)^N$. Performing an exhaustive search to compute the optimal Nash equilibrium over this exponentially sized joint strategy space is computationally infeasible.

Therefore, we propose a heuristic iterative algorithm, referred to as the Smart PsI Allocation (SPA) algorithm, to efficiently compute the equilibrium allocation (Algorithm 1). The SPA algorithm takes the set of N AVs V and M available PsIs as input, initiating with an empty allocation where no AVs are assigned PsIs. It then iteratively assigns PsIs to each AV $v_i \in V$ based on a greedy selection of the PsI(s) that maximize v_i's utility given prior assignments, repeating this process across all AVs until convergence. We empirically evaluate the quality of the approximate equilibrium computed by our proposed SPA algorithm in Section IV.

Algorithm 1 SPA: Smart PsI Allocation

```
1:  for i ← 1 to N  do                          ▷ PsI initialization
2:      numPsI ← rand(0, 2)                     ▷ The number of PsI's
3:      for j ← 0 to numPsI  do
4:          PsIs[i] ← rand(1, M)                ▷ Random allocation
5:      end for
6:  end for
7:  count ← N
8:  while count > 0 do
9:      count ← 0
10:     S ← {v_1, v_2, ..., v_N}                ▷ Initialization
11:     ts ← [PsIs]                             ▷ Transition sequence
12:     while S is not empty do
13:         v_i ← pop random AV from S
14:         V_i^1 ← PsIs[v_i]
15:         V_i^* ← getBestPsI(v_i)
16:         if V_i^* \ V_i^1 ≠ φ then
17:             count ← count + (|V_i^*| − |V_i^1|)
18:             PsIs[v] ← V_i^*
19:             SC_i ← successors(v_i)
20:             if (|SC_i| ≠ 0) then
21:                 S ∪ SC_i
22:             end if
23:             ts.append(PsIs)
24:         end if
25:     end while
26:     if ts[0] = ts[end] then                 ▷ Cycle detected
27:         R ← breakCycle(transitionSequence)
28:     end if
29: end while
```

1) OVERVIEW OF SPA

Next, we explain the different components and sub-components of the smart PsI allocation algorithm. Lines 1 to 5 in Algorithm 1 randomly assign PsIs to vehicles. Here, each vehicle can be assigned zero, one, or two PsIs.

Inside the outer loop in line 10, we set the set S containing all the vehicles for which the optimal PsI allocation remains to be determined. Let us define ts in line 11 as the array representing the current PsIs allocations (transition sequences) for all vehicles, formulated as $ts = (V_1^1, V_2^1, \ldots, V_n^1)$, where V_i^1 corresponds to the current PsIs allocation for vehicle v_i. The subsequent step involves the random selection of a vehicle, v_i, from set S. For this selected vehicle, the optimal set of PsIs, labeled as V_i^*, is calculated. This calculation takes into account the current allocation of PsIs for other vehicles as shown in Equation (9). if there is

a discrepancy between V_i^1, the current set of PsIs allocated to the vehicle v_i, and the newly computed set V_i^*, then the allocation for vehicle v_i is then updated to V_i^*.

Every time the allocation for a vehicle v_i is updated, the utility of at most four vehicles may be updated, too. Specifically, an increment in the utility is observed for the vehicle that subsequently arrives at the PsIs denoted by V_i^1 following the arrival of v_i. Conversely, there is a decrement in utility for vehicles arriving subsequently at PsIs encompassed within V_i^* in relation to v_i. We call these vehicles the successors of v_i, symbolized as SC_i. Thereby, we need to re-evaluate the optimal PsI allocation for every vehicle v_j that is a member of SC_i. At this juncture, the set SC_i is incorporated into the set S. It is pertinent to note that this inclusion process yields no changes if SC_i is already a constituent of S, considering that S is structured as a set.

2) STOPPING CRITERIA

Reaching a Nash equilibrium in the context of PsI allocation means that the allocation for each vehicle is in an optimal state with respect to the allocations of all other vehicles. Here, we will show that the achievement of such an equilibrium leads to the termination of the algorithm outer while-loop. Initially, the set S is populated with all vehicles, as presented in line 10. Thus, once a vehicle v_i is extracted from S, it can be inferred that its current assignment V_i^1 continues to be the optimal one. This suggests that the allocation for v_i remains constant, precluding the addition of any new vehicle to S. Over time, this process results in the depletion of the set S, accompanied by no modifications in the assignments. This depletion, in turn, causes the variable *count* to diminish to zero, thereby fulfilling the criteria for concluding the outer loop.

In certain scenarios, the presence of a Nash equilibrium may not be a given. Under such circumstances, the convergence of the iterative algorithm, as detailed in Algorithm 1, cannot be assured. Next, we will formalize the aforementioned algorithm and describe the underlying reasons for the lack of convergence. Furthermore, we will propose a methodology that addresses the convergence issues associated with the algorithm.

3) SPA FORMALIZATION

We represent the iterative mechanism employed in the **SPA** algorithm in terms of forward propagation within a directed graph. Let's $\mathcal{S} = (V_1^*, V_2^*, \ldots, V_N^*)$ be the set of ordered tuples, each corresponding to a specific PsI allocation configuration. Given that each AV may be assigned to any PsI, two or potentially not assigned at all, the number of states in $\mathcal{S}$ is $(M(M-1)+M+1)^N$. Let $G = (\mathcal{S}, E)$ be a directed graph, where E represents the set of directed edges. Here, an edge $(\phi_a, \phi_b) \in E$ if the tuples ϕ_a and ϕ_b differ solely at a single specified location, specifically the i^{th} location.

Additionally, ϕ_{bi} is identified as the optimal PsI for the AV v_i. This optimality is determined by Equation (9), and is contingent upon all other PsI allocations $V_j^*, j \neq i$ present in both ϕ_a and ϕ_b. This theoretical representation as a graph facilitates a structured analysis of the iterative process inherent in the SPA algorithm.

Example 1: In this scenario, we have $N = 3$ (number of vehicles) and $M = 3$ (number of PsIs), consider a set of vehicles v_1, v_2, v_3 and a corresponding set of PsIs t_1, t_2, t_3. Here, the state $\phi_a = (\{t_1\}, \{t_1, t_2\}, \{t_2\})$, suggests that vehicles v_1, v_2, and v_3 are allocated PsIs t_1, $\{t_1, t_2\}$, and t_2, respectively. Now, given the assignments for v_1 and v_2, let's assume that the optimal assignment for v_3 is determined to be t_3. Then, we have a new state $\phi_b = (\{t_1\}, \{t_1, t_2\}, \{t_3\})$ where ϕ_a and ϕ_b differ solely at one position.

In the graph-theoretic representation of this system, the tuple (ϕ_a, ϕ_b) is characterized as an edge within the directed graph. This edge corresponds to a state transition, indicative of a change in the PsI allocation for one vehicle, in this case, v_3, while maintaining the allocations for v_1 and v_2. This method of analysis allows for a structured examination of the PsI allocation dynamics within the system.

In the context of Algorithm 1 and the corresponding graph representation, the initial for-loop (lines 1 to 5) selects a random state within the graph. Lines 10 to 12 randomly select a v_i (equivalent to choosing a random location within the state tuple). This process is followed by the determination of the optimal PsI for that v_i, represented as V_i^*. Then, lines 16 to 18 focus on associating the selected vehicle v_i with its newly identified optimal PsI, V_i^*. This association results in the alteration of the PsI assignment for the specific vehicle v_i, while concurrently maintaining the existing assignments for all other vehicles. Such a modification in the state mirrors a transition within the directed graph G, characterized by the traversal across a single edge in a forward direction. This traversal corresponds to a step towards optimizing the overall PsI allocation within the system, adhering to the algorithm's design to incrementally approach an optimal state configuration.

4) NASH EQUILIBRIUM

While Section III-C2 offers an intuitive rationale for the termination of the algorithm at a Nash equilibrium, this section formally proves this claim.

Let $G = (\mathcal{S}, E)$ be a directed graph, where $\mathcal{S}$ is the set of states, and E is the set of edges. Within this graph, the *in-degree* of a vertex $\phi \in \mathcal{S}$, denoted as $d_i(\phi)$, is defined as the number of edges that converge into ϕ. Formally, it is the number of edges $(a, b) \in E$, where $b = \phi$. Conversely, the *out-degree* of ϕ, symbolized as $d_o(\phi)$, is the number of edges leaving out from ϕ. These are the edges $(a, b) \in E$, where $a = \phi$.

The central assertion to be proven is that the algorithm terminates if and only if a Nash equilibrium is reached, which corresponds to a state in the graph G with properties linked to its in-degree and out-degree. Next, we will establish the necessary and sufficient conditions for the algorithm's termination at a Nash equilibrium.

Lemma 1: A state ϕ_e is a Nash equilibrium if and only if the *out-degree* of ϕ_e is equal to zero.

Proof: Assume ϕ_e is a Nash equilibrium, and that $d_o(\phi_e) > 0$. Then, there is an edge $e \in E$ such that $e = (\phi_e, \phi_f)$. According to the definition of the edges in the graph, ϕ_e and ϕ_f differ in exactly one location, say i, and that

$$u_i\big(\phi_{fi}, \{\phi_{ej}, j \neq i\}\big) > u_i\big(\phi_{ei}, \{\phi_{ej}, j \neq i\}\big)$$

Now, by definition of Nash Equilibrium, we have

$$\phi_{ei} = \arg\max_{t_k, t_p} u_i\big(t_k, t_p, \{\phi_{ej}, j \neq i\}\big),$$

which leads to a contradiction. Thus, if ϕ_e is a Nash equilibrium, then $d_o(\phi_e) = 0$.

Now, for any vertex $\phi_e \in \Phi$, assume that $d_o(\phi_e) = 0$. This means that for each i, ϕ_{ei} is the best assignment for v_i given all other assignments. Otherwise, there would have been an edge starting at ϕ_e, making its out-degree positive. This means that ϕ_e is a Nash equilibrium.

Whenever the algorithm reaches a state with *out-degree* equal to zero, it will have been allocated its optimal PsIs. Under such circumstances, the if-conditional statement in line 16 will consistently be evaluated as false, leading to the cessation of the algorithm's execution.

Conversely, if a Nash equilibrium is not reached, it is because the graph G possesses a cycle. This is because of the finite structure coupled with the fact that every vertex must have a minimum of one outgoing edge. In such situations, the **SPA** algorithm is susceptible to becoming entrapped within this cycle. To counteract this, **SPA** uses a subroutine designed to identify and address these cycles. The approach involves the strategic reduction of the reward parameter R to eliminate an edge within the cycle, thereby facilitating the exit from the loop. The steps dedicated to cycle detection and resolution correspond to lines 11, 26, and 27. Thus, We ensure the algorithm does not perpetually iterate within a cycle but rather progresses toward a state of optimal PsI allocation.

5) BREAKING A CYCLE

Consider the detection of a cycle $c = (e_1, e_2, \ldots, e_n)$, where edge $e_\rho = (\phi_{\rho 1}, \phi_{\rho 2})$ is in the cycle. Corresponding to edge e_ρ, let v_ρ denote the AV for which there is a change in PSI allocation from t_k to t_l. This implies that considering the allocations of all other vehicles, t_l was deemed the optimal PsI for v_ρ as per equation (9). To disrupt this edge, it is necessary to adjust the value of the reward parameter R such that t_l ceases to be the optimal PsI. Let's use the notation $u_{\rho k} = u_\rho(t_k, v_j; j \neq \rho)$ and $\delta_{\rho k} = \delta(a_{\rho k} - a^-_{\rho k}, v_j; j \neq \rho)$. The utilities are then arranged in a descending sequence: $u_{\rho l} \geq u_{\rho j_1} \geq \cdots \geq u_{\rho j_v} \geq u_{\rho k}$. Given that the costs associated with deviating to different PsIs are fixed, and considering the choices of other vehicles, the δs are constant. Consequently, the utilities $u_{\rho k}$ function as affine expressions of R.

Define R_ρ as the specific value of R at which $u_{\rho l} = u_{\rho j_1}$. By setting R to be less than R_ρ, the PsI t_{j_1} becomes the optimal choice for v_ρ as opposed to t_l, effectively eliminating the edge e_ρ from G. This procedure can be replicated for each edge in the cycle c. The appropriate R value is then set to the maximum of these R_ρs (minus a negligible quantity ϵ) to ensure the removal of precisely one edge from the cycle c, thereby disrupting it. Our simulation results show that if NE is not found using lines 1 to 25, a maximum of three cycles are found and broken before finding the NE. If NE is not found after three cycles, then it will not exist.

Thus, this section presented the **SPA** algorithm, which outputs a Nash Equilibrium allocation following Equation (8). The algorithm achieves that by traversing a directed graph until reaching a state vertex with zero outward edges. Finally, the algorithm uses a sub-routine to find cycles and break them by reducing the value of R.

D. SELECTION OF MAXIMUM REWARD

The compensation gain by an AV for sensing at a given PsI corresponds to the product $R\delta$, with $\delta \in [0, 1]$. Here, R represents the maximal reward attainable by any AV for a single measurement. The average utility of the platform, denoted as $\mathcal{U}$ and calculated via equation (1), exhibits an increasing trend with escalating values of R, achieving a peak at a specific value termed R_{max}. In scenarios where the primary objective of the platform is to maximize average utility, the optimal strategy would involve setting R equal to R_{max}. However, the total rewards disbursed by the platform are directly proportional to R. This leads to a diminishing rate of return, represented as $\mathcal{U}/R$, as R increases. If the platform prioritizes this rate of return, the determination of R would then be contingent upon a predefined threshold. Additionally, the existence of a Nash equilibrium, as described in equation (7), may not be assured at large values of R. The presence of a Nash equilibrium is crucial to guarantee adherence from self-interested, rational players (AVs), thereby rendering it a significant factor in the decision-making process regarding the setting of R. It is also important to note that while the reward the platform determines R, the execution of the **SPA** algorithm is undertaken by the AVs. This dichotomy suggests a degree of cooperation between the two entities in establishing the value of R. This cooperative aspect is vital in ensuring that the algorithm's implementation aligns with the overarching objectives of the platform, balancing utility maximization with economic efficiency.

IV. PERFORMANCE EVALUATION

Here, we evaluate the performance of the proposed incentive mechanism. We divide the evaluation process into two components. The first part evaluates a set of metrics in a scenario where vehicles go from source to destination, and they are allowed to deviate from their pre-planned trajectory to visit at most one PsI. The second part analyses the effect on the evaluated metrics of allowing vehicles to deviate and visit at most two PSIs. In particular, we are interested in finding the trade-off in terms of participants and platform

utility versus the time complexity of allowing vehicles to deviate and visit several PSIs in the same trajectory. We are interested in evaluating the use of our method on metrics such as temporal coverage (platform utility), spatial coverage, road utilization, and average participant utility.

We run most of our experiment using two scenarios: a unit grid where vehicles' departure and arrival to destination are represented by a straight line and a second, more realistic scenario that includes real maps and the vehicular driving simulator (SUMO) [42]. The unit grid simplified environment used as proof of concept. For the scenario, we use an Open Street Map (OSM) from the city of Cologne, Germany, which has drivable roads to allow variation in routing possibilities.

The proposed incentive mechanism is modeled as a non-cooperative game with two players: Participant vehicles or AVs and the platform. Here, both players have divergent objectives. The platform's goal is to maximize its utility, namely, to get samples of high quality (temporal coverage), while the participant's goal is to maximize their monetary utility. Thus, we want to find out if these objectives are aligned, namely if the consecutive of one party's goal incentivizes the consecutive of the other party's objective.

To evaluate the performance of the proposed approach, we introduce a naive reward mechanism (**N**) for the platform and a greedy algorithm (**G**) for the AVs, and we will refer to this combination as (**NG**). The reward proposed mechanism (time-dependent sampling) is denoted by **V**. Under the **N** reward mechanism, the platform rewards R for any sample taken by the AVs regardless of the sampling time. In the **G** algorithm, the vehicles select the PsI with the lowest cost and a positive utility. Finally, (**S**) refers to the participants' utility that results from using the **SPA** algorithm. Note that the algorithm **G** produces a Nash equilibrium for the AVs under **N** reward mechanism. Thus, evaluate the combination platform reward proposed and utility from greedy sampling (**VG**), platform reward proposed and participant using **SPA** algorithm (**VS**), and finally, naive platform and greedy participant (**NG**).

Thus, The efficacy of this program depends on satisfying the following critical issues:

Temporal Coverage: The program must demonstrate its capacity to enable the platform to secure high-caliber samples. Additionally, it should offer a mechanism through which the platform can enhance the quality of these samples by allocating additional financial resources.

Participant Utility: It is imperative to ensure that the AVs receive sufficient motivation to adopt the proposed SPA methodology. This adoption aims to maximize their utility, striking a balance between program participation and economic gain.

Systemic Incentives: A key aspect of the program is the alignment of incentives between the platform and the AVs. The core hypothesis posits that the AVs, while pursuing their self-interest and maximizing their utility, inadvertently contribute to the utility of the platform. This synergy between individualistic goals and collective benefits underpins the program's potential success.

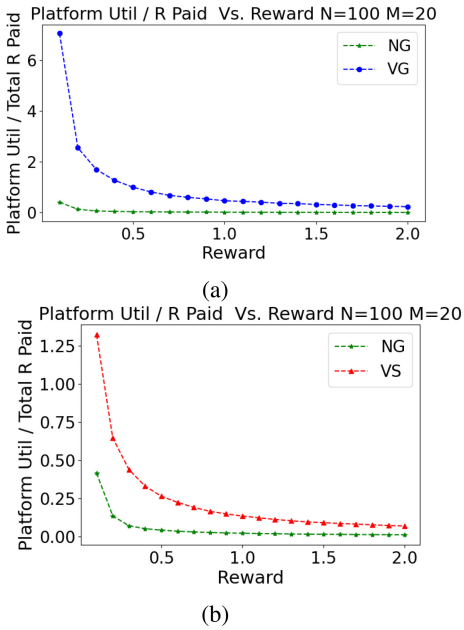

FIGURE 3. Figures show that even when the AVs shift from G an algorithm to the SPA algorithm, the return on investment for the platform is superior when V rewards are used compared to N.

A. TEMPORAL COVERAGE

In this experiment, we compare two distinct reward mechanisms: The **V**-based mechanism (hereafter referred to as **V**) and the **N**-based mechanism (hereafter referred to as **N**). The evaluated metric here is platform utility per unit of reward disbursed. This comparison is graphically represented in Figure 3(a), where the y-axis corresponds to the average platform utility $\mathcal{U}$ relative to the reward amount expended, and the x-axis to varying values of R. Figure 3(a) shows that the **V** reward mechanism yields a better rate of return when compared to the **N**. In these simulations, the AVs are running the G algorithm for PSI allocation. Figure 4 shows the platform's ability to enhance the quality of data samples by increasing financial investment, specifically under the **V** reward mechanism. It is also noticeable that $\mathcal{U}$ exhibits a positive correlation with R. Additionally, the figure underscores the inability of the **N** mechanism to exert similar control over the quality of samples, a capability evidently present in the **V** mechanism. This comparative analysis provides valuable insights into the effectiveness of different reward structures in influencing the utility and operational efficiency of the platform, especially in the context of data quality and economic expenditure.

B. PARTICIPANT UTILITY

In Section IV-A, we demonstrate the advantage for the platform when using the **V** reward mechanism while the AVs utilize the **G** algorithm. Here the transition from the **G**

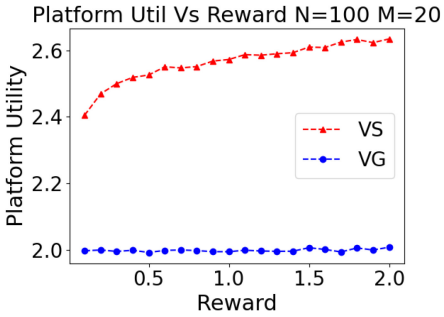

(a) Unit Grid

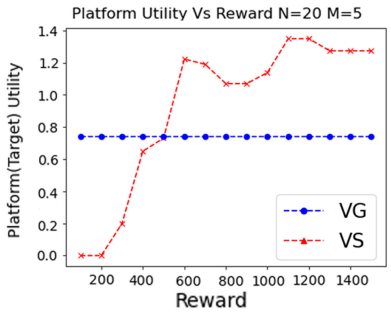

(b) Map

FIGURE 4. Show that platform utility $\mathcal{U}$ exhibits an increasing behavior for increasing values of R, showing the platform's capacity to enhance the acquisition of quality data by investing more resources when using the V reward mechanism. Here, the blue line corresponds to the N reward mechanism.

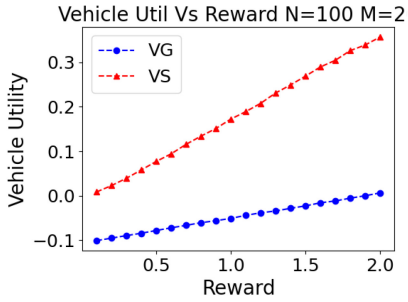

(a)

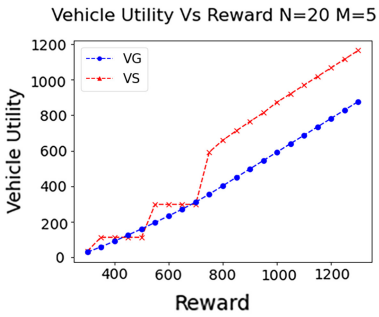

(b)

FIGURE 5. Average participant Utility: G vs SPA allocation approaches both using sampling-dependent V for unit-grid (a), and map (b).

algorithm to **SPA** algorithm requires global knowledge to be shared between the AVs and the platform about the source and destination locations of all AVs, along with the AVs to dedicate computational resources to the **SPA** algorithm.

In this experiment, we contrast the average participants' utility when using the Greedy allocation approach **G** (blue line) versus the smart allocation algorithm **SPA** (red line) for increasing values of R. In both cases, the **V** sampling time-dependent approach is used. Figure 5 in both the unit grid and map scenarios shows a substantial enhancement in average participant utility with the application of the **SPA** algorithm. This will incentivize participants to transition from the **G** to **SPA** approach.

C. SYSTEMIC INCENTIVES

Figure 6 shows the alignment between the objectives of the platform and participants. Here, the rows constitute the platform options in terms of sampling-based offered reward, namely **V** or **N**, and the columns are the participants' options in terms of allocation **G** and **SPA (S)**. Note, that when the platform is using **N** reward mechanism, both **G** and **S** algorithms lead to the same result.

As Section IV-A concludes, the implementation of a **V** reward mechanism by the platform significantly enhances its return on investment. This will incentivize the platform to transition from **N** to the **V** reward approach. In addition, Section IV-B reveals that the adoption of the **V** reward mechanism concurrently improves the utility of participants. This increment is significant when AVs transition from the **G** algorithm to the more robust **S** approach. Thus, driven by self-interest, both the platform and the AVs naturally transition from the initial state (**N**, **G**) to the (**V**, **S**) state. Figure 3(b) graphically shows the enhanced return on investment for the platform when the system migrates from its foundational state (**N**, **G**) to the equilibrium state of (**V**, **S**). This transition shows the mutual benefits reach by both the platform and the AVs in adapting to the **V** reward mechanism and the **S** algorithm. Figure 7 shows an increase in the sample entropy of the PsI utilities. This increase is attributed to the transition of AVs from the **G** to the **S** algorithm. This results in an improvement of **spatial coverage**, which results from a reduction in the variability of sample quality across different PsIs. This phenomenon aligns the objectives of both the platform and the AVs, with each entity benefitting from self-interested actions.

D. ROAD UTILIZATION

Here, evaluate the performance of our **SPA** algorithm versus the **G** algorithm in terms of road utilization. This is important metric that shows how a reward mechanism may spread a city traffic avoiding traffic jams allowing a better use the road network. Figure 8 shows the set of trajectories resulting from **G** and **SPA** algorithms. We use Open Street Maps from Cologne Germany, and SUMO traffic simulator for trajectory

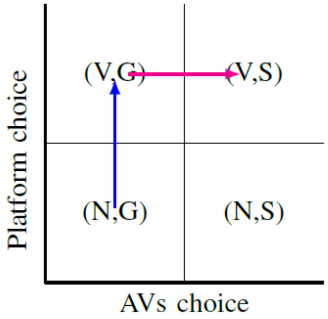

FIGURE 6. Figure shows the incentive drives for the players involved. The platform is incentivized to use a well-designed reward mechanism to improve return on investment, and the AVs are incentivized to share information and use the target allocation algorithm.

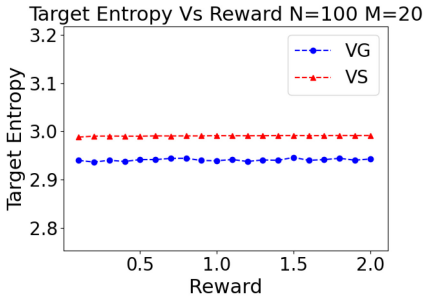

(a)

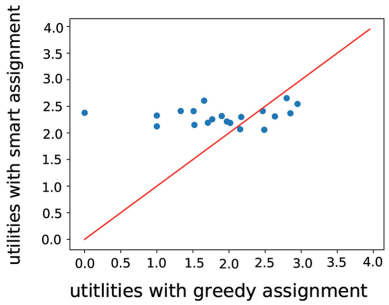

(b)

FIGURE 7. Spatial coverage: figure (a) shows that the sample entropy of PsI utilities increases when AVs switch from G algorithm to SPA algorithm. Figure (b) a scatter plot of PsI utilities in the case of G algorithm (x-axis) vs SPA algorithm (y-axis). Note that the spread in the PsI utilities is much less in the SPA case.

generation. Figure 8 (b) shows that vehicles using the **SPA** algorithm use a greater portion of the city roads.

SPA algorithm.

In this experiment we explore the effect of reward or platform investment on road utilization. We normalize road utilization values by baseline. We noted that for reward values less 700 both **SPA** and **G** perform at the same level. This could be explained by the fact that the decision factor of whether or not deviate from the pre-planned trajectory and sampling from a PSI is cost. We also see that for reward values greater than 700 AVs **SPA** outperforms **G** in terms of road utilization. This explained by the fact that AVs start to get a positive utility, and therefore visiting remote PSIs.

(a) Greedy

(b) Smart

FIGURE 8. Road Utilization.

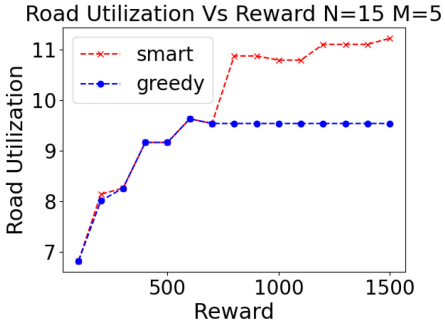

FIGURE 9. Road utilization SPA vs G on the Map.

E. COMPARING ONE VS TWO VEHICLES TO PSI ALLOCATION

This section holds further experimental validation of the vehicle crowd-sensing algorithm. Experiments were performed increasing the number of vehicles in a given scenario and comparing the results of allowing vehicles to stop at up to 2 PsIs against the single PsI allocation results. As the number of vehicles was increased, analysis was conducted over platform reward, platform utility, and vehicle utility.

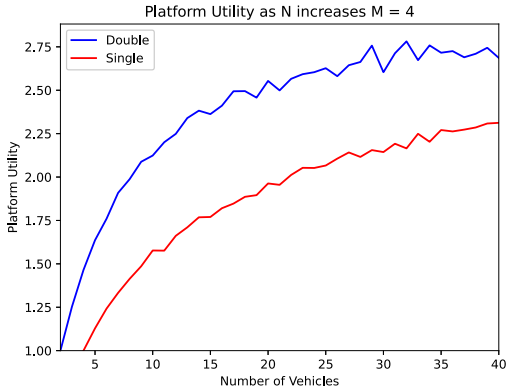

FIGURE 10. Platform Utility.

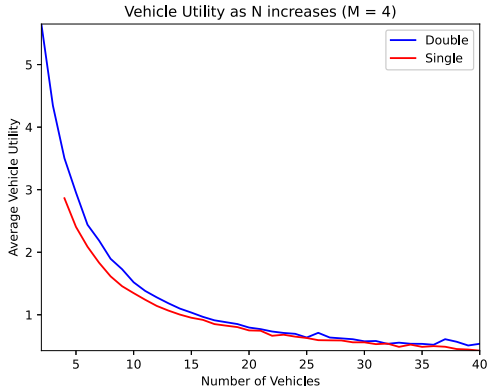

FIGURE 11. Average Vehicle Utility.

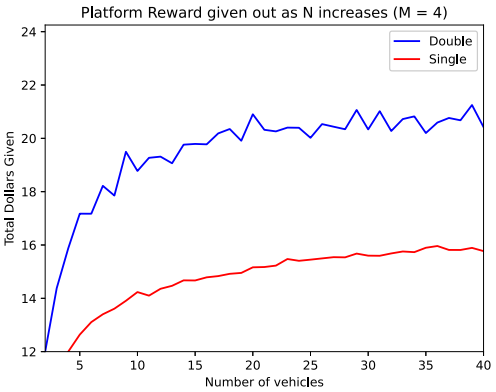

FIGURE 12. Platform Reward.

These metrics, as defined below, hold the same definition as in the single target allocation paper.

F. PLATFORM UTILITY

The platform utility is defined as the quality of all PsI's samples in regards to maximizing temporal coverage. This is found using entropy to find the individual target utilities and calculating the average of all target's utilities. An individual target's utility can be found by first collecting all of this PsI's vehicle arrival times. The observation period is set to start at zero, while the ending of the period is at the final vehicle's arrival time in addition with the average of all arrival times. Observing the interval times between these sampled times, these interval times between samples can be normalized by dividing by the number of intervals. This creates probabilities that can be used within the desired entropy function. An entropy function is used as the utility function among these probabilities to calculate a target's utility.

As shown in the figure above, the platform utility increases as the number of vehicles increases. This result is due to the number of samples increasing in a uniformly timed manner, outputting a higher target utility. The spread intervals between samples is encouraged among the vehicles by rewarding vehicles for arriving furthest from the last arrival time. Observing the single and double target allocation, the resulting platform utility is considerably higher when allowing vehicles to stop at 2 PsIs. This metric can then be compared to the following metrics to determine whether stopping at two PsI's would be advantageous.

G. AVERAGE VEHICLE UTILITY

The vehicle utility is defined as the reward given to the vehicle for sampling new data at specific targets subtracted by the cost taken to deviate from the vehicle's direct destination path. The reward given out is calculated by multiplying the maximum reward by a multiplier in the range of [0, 1]. This multiplier, δ, increases the longer the interval between the previous vehicle's arrival time and the observed vehicles arrival time. The cost is calculated by multiplying another multiplier, α, by the difference of the length of source, target 1, target 2, to destination, by the length of source to destination. The vehicle utilities are averaged to display the shown value above. As shown, individual vehicles utility decreases as the number of vehicles increases. This is a result of smaller rewards being handed out with closer sampled intervals, arrival times. This, along with the figure of platform utility, shows that as the platform utility increases, the individual vehicle utility decreases. This trend applies similarly to both the single and double target allocation scenarios. While the double target allocation starts the scenario with a much higher average vehicle utility, the graph immediately starts to match with the single target allocation as vehicles increase.

$$u_i(t_k) = R * \delta - \alpha * (|s_i * t_k * d_i| - |s_i * t_i|) \tag{11}$$

H. PLATFORM REWARD

The platform reward is calculated by summing up the individual rewards given to each vehicle for sampling data at a PsI. As shown above, this value, in both allocation types, increases as the number of vehicles increases. This positive rate of change's effect on the total dollars given diminishes in return as the sampling intervals become smaller. The smaller the interval between arrival times, the less reward is given to the following vehicle. Platform reward increased once vehicles were open to stop at 2 PsIs, which resulted in the increased platform utility shown earlier.

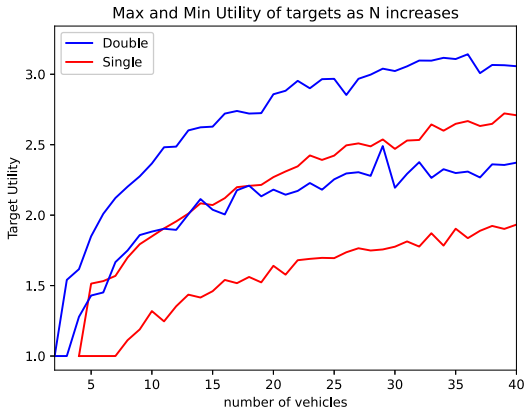

FIGURE 13. Minimum and Maximum Target Utility.

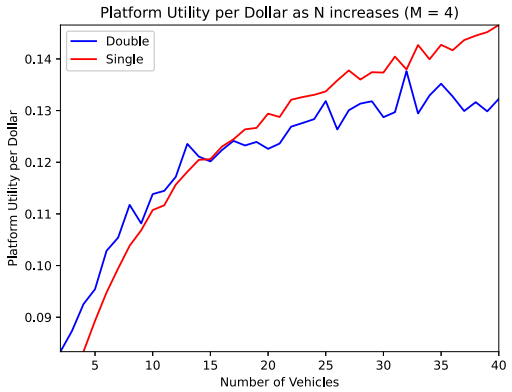

FIGURE 14. Platform Utility Per Dollar.

I. MINIMUM AND MAXIMUM TARGET UTILITY

The maximum and minimum utility of targets are found through the same process as the platform utility, but taking the maximum and minimum of target utilities, instead of the average. An important observation is that the difference between the maximum and minimum utility doesn't change drastically as the number of vehicles increases. This would infer that there isn't a specific PsI that is greatly suffering compared to the target's with higher utilities.

J. PLATFORM UTILITY PER DOLLAR

The Platform Utility per Dollar represents how the platform's utility correlates with the platform reward amount given out. The value is calculated by simply dividing the platform utility with the platform reward. An interesting observation is that as the number of vehicles increases, the single target allocation overtakes the double target allocation. The positive rate of change of the double target allocation curve decreases much sooner than the single target allocation. While the platform utility of the double target allocation was considerably higher, the platform reward also increased, leaving the actual result, as vehicles increase, to be less efficient than simply using single target allocation.

V. CONCLUSION

This paper presents an incentive mechanism for VCS, focusing on maximizing temporal coverage. We model the proposed mechanism as a non-cooperative game in which the players are participants' vehicles and the platform. Here, the platform sets PsIs at different locations and the corresponding budget R per sensing task, and the participants attracted by those rewards deviate from their pre-planned trajectories to collect data from the PsIs that maximize their utility. Here, the utility of corresponds to a well distributed set of samples in time (temporal coverage), quality sensing data (QoSD), namely a set of samples with high entropy. On the other hand, participants utility corresponds to monetary magnitude which is maximized when sampling a time-dependent approach. We show that goals of the platform and participants are aligned, namely the maximization of one party utility incentives the maximization of the other party utility. Through extensive simulations, we show how our outperforms a greedy approach in terms of QoSD, average vehicle utility, spatial coverage, and road utilization. Our results underscore that the objectives of self-interested players align, and the equilibrium state benefits both the platform and the AVs. We also compare the benefits and drawbacks of allow vehicles to deviate one or more time from their pre-planned trajectories.

REFERENCES

[1] A. Chakeri, X. Wang, and L. G. Jaimes, "A vehicular crowdsensing market for AVS," *IEEE Open J. Intell. Transp. Syst.*, vol. 3, pp. 278–287, 2022.

[2] H. Chintakunta, J. Kahr, and L. Jaimes, "A vehicular crowd-sensing incentive mechanism for temporal coverage," in *Proc. IEEE 18th Annu. Consum. Commun. Netw. Conf. (CCNC)*, 2021, pp. 1–8.

[3] M. W. Beck, M. C. Burke, G. E. Raulerson, S. Scolaro, E. T. Sherwood, and J. Whalen, "Coordinated monitoring of the Piney point wastewater discharge into Tampa Bay: Data synthesis and reporting," *Florida Sci.*, vol. 86, no. 2, pp. 288–300, 2023.

[4] Y.-C. Wang and G.-W. Chen, "Efficient data gathering and estimation for metropolitan air quality monitoring by using vehicular sensor networks," *IEEE Trans. Veh. Technol.*, vol. 66, no. 8, pp. 7234–7248, Aug. 2017.

[5] N. Maisonneuve, M. Stevens, M. E. Niessen, and L. Steels, "NoiseTube: Measuring and mapping noise pollution with mobile phones," in *Information Technologies in Environmental Engineering*, Heidelberg, Germany: Springer, 2009, pp. 215–228.

[6] G. Leduc et al., "Road traffic data: Collection methods and applications," Technical Note JRC 47967, Working Papers on Energy, Transport and Climate Change, Office Official Publ. Eur. Commun., Luxembourg City, Luxembourg, 2008.

[7] C. Wang, C. Li, C. Qin, W. Wang, and X. Li, "Maximizing spatial–temporal coverage in mobile crowd-sensing based on public transports with predictable trajectory," *Int. J. Distrib. Sens. Netw.*, vol. 14, no. 8, 2018, Art. no. 1550147718795351.

[8] J. V. Mena, F. Elijorde, and Y. Byun, "On the use of in-vehicle sensors for weather data collection and mapping," in *Proc. IEEE Transp. Electrific. Conf. Expo, Asia–Pacific (ITEC Asia–Pacific)*, 2019, pp. 1–6.

[9] Y. Chon, N. D. Lane, Y. Kim, F. Zhao, and H. Cha, "Understanding the coverage and scalability of place-centric crowdsensing," in *Proc. ACM Int. Joint Conf. Pervasive Ubiquitous Comput.*, 2013, pp. 3–12.

[10] D. Deng, C. K. Leung, C. Zhao, Y. Wen, and H. Zheng, "Spatial-temporal data science of COVID-19 data," in *Proc. IEEE 15th Int. Conf. Big Data Sci. Eng. (BigDataSE)*, 2021, pp. 7–14.

[11] X. Du, X. Jin, X. Yang, X. Yang, X. Xiang, and Y. Zhou, "Spatial-temporal pattern changes of main agriculture natural disasters in China during 1990–2011," *J. Geograph. Sci.*, vol. 25, pp. 387–398, Feb. 2015.

[12] T. A. Nelson, D. Duffus, C. Robertson, K. Laberee, and L. J. Feyrer, "Spatial-temporal analysis of marine wildlife," *J. Coastal Res.*, vol. 2, no. 56, pp. 1537–1541, 2009.

[13] A. S. El-Wakeel, J. Li, A. Noureldin, H. S. Hassanein, and N. Zorba, "Towards a practical crowdsensing system for road surface conditions monitoring," *IEEE Internet Things J.*, vol. 5, no. 6, pp. 4672–4685, Dec. 2018.

[14] L. G. Jaimes et al., "A generative adversarial approach for Sybil attacks recognition for vehicular crowdsensing," in *Proc. Int. Conf. Connected Veh. Expo (ICCVE)*, 2022, pp. 1–7.

[15] S. Chan and K. Leong, "An application of cyclic signature (CS) clustering for spatial-temporal pattern analysis to support public safety work," In *Proc. IEEE Int. Conf. Syst., Man Cybern.*, 2010, pp. 2716–2723.

[16] K. Han, C. Chen, Q. Zhao, and X. Guan, "Trajectory-based node selection scheme in vehicular crowdsensing," in *Proc. IEEE/CIC Int. Conf. Commun. China (ICCC)*, 2015, pp. 1–6.

[17] Y. Tong, L. Chen, and C. Shahabi, "Spatial crowdsourcing: Challenges, techniques, and applications," *Proc. VLDB Endow.*, vol. 10, no. 12, pp. 1988–1991, 2017.

[18] M. Van Exel, E. Dias, and S. Fruijtier, "The impact of crowdsourcing on spatial data quality indicators," in *Proc. GIScience Doctoral Colloquium*, Zurich, Switzerland, 2010, pp. 14–17.

[19] T. A. N. Dinh, A. D. Nguyen, T. T. Nguyen, T. H. Nguyen, and P. L. Nguyen, "Spatial-temporal coverage maximization in vehicle-based mobile crowdsensing for air quality monitoring," in *Proc. IEEE Wireless Commun. Netw. Conf. (WCNC)*, 2022, pp. 1449–1454.

[20] D. Asprone, S. Di Martino, P. Festa, and L. L. L. Starace, "Vehicular crowd-sensing: A parametric routing algorithm to increase spatio-temporal road network coverage," *Int. J. Geograph. Inf. Sci.*, vol. 35, no. 9, pp. 1876–1904, 2021.

[21] X. Xia, Y. Zhou, J. Li, and R. Yu, "Quality-aware sparse data collection in MEC-enhanced mobile crowdsensing systems," *IEEE Trans. Comput. Social Syst.*, vol. 6, no. 5, pp. 1051–1062, Oct. 2019.

[22] J. Lu, Y. Xin, Z. Zhang, X. Liu, and K. Li, "Game-theoretic design of optimal two-sided rating protocols for service exchange dilemma in crowdsourcing," *IEEE Trans. Inf. Forensics Security*, vol. 13, pp. 2801–2815, 2018.

[23] L. Xue, C. Sun, D. Wunsch, Y. Zhou, and F. Yu, "An adaptive strategy via reinforcement learning for the prisoner's dilemma game," *IEEE/CAA J. Automatica Sinica*, vol. 5, no. 1, pp. 301–310, Jan. 2018.

[24] W. Xu et al., "Internet of Vehicles in big data era," *IEEE/CAA J. Automatica Sinica*, vol. 5, no. 1, pp. 19–35, Jan. 2018.

[25] K. Kong, J. Xu, M. Xu, L. Tu, Y. Wu, and Z. Chen, "Trajectory query based on trajectory segments with activities," in *Proc. 3rd ACM SIGSPATIAL Workshop Smart Cities and Urban Analytics*, 2017, p. 2.

[26] L. Sun, M. H. Karwan, and C. Kwon, "Path-based approaches to robust network design problems considering boundedly rational network users," *Transp. Res. Rec.*, vol. 2673, no. 3, 2019, Art. no. 361198119835807.

[27] D. Yang, G. Xue, X. Fang, and J. Tang, "Crowdsourcing to smartphones: Incentive mechanism design for mobile phone sensing," in *Proc. 18th Annu. Int. Conf. Mobile Comput. Netw.*, 2012, pp. 173–184.

[28] Z. He, J. Cao, and X. Liu, "High quality participant recruitment in vehicle-based crowdsourcing using predictable mobility," in *Proc. IEEE Conf. Comput. Commun. (INFOCOM)*, 2015, pp. 2542–2550.

[29] S. Xu, X. Chen, X. Pi, C. Joe-Wong, P. Zhang, and H. Y. Noh, "Incentivizing vehicular crowdsensing system for large scale smart city applications," in *Proc. Sens. Smart Struct. Technol. Civil, Mech. Aerosp. Syst.*, 2019, Art. no. 109701C.

[30] O. Urra and S. Ilarri, "Spatial crowdsourcing with mobile agents in vehicular networks," *Veh. Commun.*, vol. 17, pp. 10–34, Jun. 2019.

[31] Y. Chen, P. Lv, D. Guo, T. Zhou, and M. Xu, "Trajectory segment selection with limited budget in mobile crowd sensing," *Pervasive Mobile Comput.*, vol. 40, pp. 123–138, Sep. 2017.

[32] Y. Kim, D. Gergle, and H. Zhang, "Hit-or-wait: Coordinating opportunistic low-effort contributions to achieve global outcomes in on-the-go crowdsourcing," in *Proc. CHI Conf. Human Factors Comput. Syst.*, 2018, p. 96.

[33] G. Fan et al., "Joint scheduling and incentive mechanism for spatio-temporal vehicular crowd sensing," *IEEE Trans. Mobile Comput.*, vol. 20, no. 4, pp. 1449–1464, Apr. 2021.

[34] L. L. L. Starace, F. R. Di Torrepadula, S. D. Martino, and N. Mazzocca, "Vehicular crowdsensing with high-mileage vehicles: Investigating spatiotemporal coverage dynamics in historical cities with complex urban road networks," *J. Adv. Transp.*, vol. 2023, p. 15, May 2023.

[35] X. Zhu, S. A. Samadh, and T.-Y. Yu, "Large scale active vehicular crowdsensing," in *Proc. IEEE Veh. Technol. Conf. VTC*, 2018, pp. 1–5.

[36] V. S. Dasari, B. Kantarci, M. Pouryazdan, L. Foschini, and M. Girolami, "Game theory in mobile crowdsensing: A comprehensive survey," *Sensors*, vol. 20, no. 7, p. 2055, 2020.

[37] Z. Wang et al., "Heterogeneous incentive mechanism for time-sensitive and location-dependent crowdsensing networks with random arrivals," *Comput. Netw.*, vol. 131, pp. 96–109, Feb. 2018.

[38] L. Xiao, T. Chen, C. Xie, H. Dai, and H. V. Poor, "Mobile crowdsensing games in vehicular networks," *IEEE Trans. Veh. Technol.*, vol. 67, no. 2, pp. 1535–1545, Feb. 2018.

[39] E. Wang, Y. Yang, J. Wu, and H. Wang, "Multi-round bidding strategy based on game theory for crowdsensing task," in *Proc. 12th Int. Conf. SpaCCS Security, Privacy, Anonymity Comput., Commun., Storage*, Atlanta, GA, USA, 2019, pp. 196–210.

[40] L. Duan, T. Kubo, K. Sugiyama, J. Huang, T. Hasegawa, and J. Walrand, "Motivating smartphone collaboration in data acquisition and distributed computing," *IEEE Trans. Mobile Comput.*, vol. 13, no. 10, pp. 2320–2333, Oct. 2014.

[41] T. M. Cover, *Elements of Information Theory*. New York, NY, USA: Wiley, 1999.

[42] D. Krajzewicz, J. Erdmann, M. Behrisch, and L. Bieker, "Recent development and applications of sumo-simulation of urban mobility," *Int. J. Adv. Syst. Meas.*, vol. 5, nos. 3–4, pp. 128–138, 2012.